Cell

Crystal Structure of the Catalytic α Subunit of E. coli Replicative DNA Polymerase III

Meindert H. Lamers,[1] Roxana E. Georgescu,[3] Sang-Gyu Lee,[3] Mike O'Donnell,[3] and John Kuriyan[1,2,*]
[1] Howard Hughes Medical Institute, Department of Molecular and Cell Biology and Department of Chemistry, University of California, Berkeley, CA 94720, USA
[2] Physical Biosciences Division, Lawrence Berkeley National Laboratory, Berkeley, CA 94720, USA
[3] Laboratory of DNA Replication, Howard Hughes Medical Institute, The Rockefeller University, New York, NY 10021, USA
*Contact: kuriyan@berkeley.edu
DOI 10.1016/j.cell.2006.07.028

SUMMARY

Bacterial replicative DNA polymerases such as Polymerase III (Pol III) share no sequence similarity with other polymerases. The crystal structure, determined at 2.3 Å resolution, of a large fragment of Pol III (residues 1–917), reveals a unique chain fold with localized similarity in the catalytic domain to DNA polymerase β and related nucleotidyltransferases. The structure of Pol III is strikingly different from those of members of the canonical DNA polymerase families, which include eukaryotic replicative polymerases, suggesting that the DNA replication machinery in bacteria arose independently. A structural element near the active site in Pol III that is not present in nucleotidyltransferases but which resembles an element at the active sites of some canonical DNA polymerases suggests that, at a more distant level, all DNA polymerases may share a common ancestor. The structure also suggests a model for interaction of Pol III with the sliding clamp and DNA.

INTRODUCTION

Replicative DNA polymerases are multiprotein holoenzyme complexes that carry out highly processive DNA replication during cell division, with tight coordination of leading and lagging strand synthesis (Johnson and O'Donnell, 2005; Waga and Stillman, 1998). The replicative polymerase of *E. coli*, DNA Polymerase III, is a ten subunit complex, with the 130 kDa α subunit (referred to as Pol III in this paper) being the catalytic DNA polymerase subunit. Although much is now known about the structures of DNA polymerases in general (Brautigam and Steitz, 1998; Rothwell and Waksman, 2005), it is remarkable that the catalytic subunit of Pol III is of completely unknown structure.

One of the most striking aspects of the Pol III holoenzyme is its ability to move with the advancing replication fork at speeds approaching 1000 bp/s, with the catalytic subunit making only 1 error in $\sim 10^5$ steps prior to proofreading (Bloom et al., 1997). The speed of *E. coli* DNA Pol III may be contrasted with that of the eukaryotic replicative polymerases, which operate at replication forks that move ~20 times slower (Raghuraman et al., 2001). In *E. coli* and other Gram-negative bacteria a proofreading 3′-5′ exonuclease forms a separate subunit named ε, which is bound tightly to Pol III. Gram-positive bacteria have two DNA polymerases that are related to *E. coli* Pol III. One of these, Pol C, is the replicase and has the 3′-5′ exonuclease activity as part of the same polypeptide chain as the DNA polymerase (Huang et al., 1997). The other polymerase is more closely related to *E. coli* Pol III in its domain organization, but its role in chromosomal replication is unclear (Bruck et al., 2003).

The sequences of Pol III and Pol C share no detectable similarity to any DNA polymerase of known structure. Particularly surprising is the lack of sequence similarity to the replicative polymerases in eukaryotes, such as human DNA Pol δ and ε and the archaeal replicative DNA polymerases (Braithwaite and Ito, 1993). These polymerases are homologs of bacterial DNA Pol II, which does not function in chromosomal replication (Bonner et al., 1990). Although the structures of Pol δ and Pol ε remain unknown, crystal structures have been determined for the homologous DNA polymerase of bacteriophage RB69 (Franklin et al., 2001; Wang et al., 1997), as well as for archaeal DNA polymerases (Hopfner et al., 1999; Rodriguez et al., 2000; Zhao et al., 1999).

All replicative DNA polymerases acquire high processivity by the coupling of the catalytic subunits to sliding DNA clamps that encircle DNA (Kong et al., 1992; Krishna et al., 1994). Sliding clamps are loaded onto DNA by the ATP-dependent clamp loader complexes, the subunits of which are related in sequence and in structure in bacteria, archaea, and eukaryotes (Bowman et al., 2005). The conservation of the clamp loader subunits suggests that the mechanisms for processive replication in all three

domains of life have diverged from that of a common ancestral replication complex.

This view is countered by the fact that, in addition to the apparent unrelatedness of the replicative polymerases, the bacterial primase enzymes that are critical for Okazaki fragment synthesis are unrelated to those in eukaryotes and archaea (Leipe et al., 1999). These points of distinction have led to the suggestion that DNA replication may have evolved twice independently after divergence from the last common ancestor of the bacteria on the one hand and the eukaryotes and archaea on the other (Forterre, 2006; Leipe et al., 1999).

DNA polymerases resemble a right hand in overall shape, with Palm, Fingers, and Thumb domains (Brautigam and Steitz, 1998; Rothwell and Waksman, 2005). The three domains form a deep cleft, with the active site located within the Palm domain at the bottom of the cleft. The Fingers domain binds the incoming nucleotide, while the Thumb domain guides the nascent DNA duplex as it leaves the active site (Doublie et al., 1998; Eom et al., 1996; Franklin et al., 2001; Kiefer et al., 1998; Li et al., 1998; Pelletier et al., 1994).

DNA polymerases can be divided into two main groups, the A/B/Y families and the X family, based on the topology of the secondary structural elements and the location of catalytic residues in the Palm domain. The A family polymerases include *E. coli* DNA Pol I, T7 DNA polymerase, and Taq polymerase (Brautigam and Steitz, 1998; Rothwell and Waksman, 2005). The eukaryotic replicative DNA polymerases Pol δ and Pol ε belong to the B family of polymerases. The Y family members, such as bacterial DinB and UmuC, are involved in movement of the replication machinery past lesions in the template (Goodman, 2002). The catalytic centers of HIV reverse transcriptase and bacteriophage T7 RNA polymerase are similar to that of A/B/Y polymerases (Brautigam and Steitz, 1998; Rothwell and Waksman, 2005). We refer to the A/B/Y family members as canonical DNA polymerases.

The X family DNA polymerases, of which Pol β is the prototype, are structurally different from the A/B/Y polymerases in the organization of the active site in the Palm domain. These polymerases belong to the superfamily of nucleotidyltransferases (Aravind and Koonin, 1999; Holm and Sander, 1995), many of which are involved in RNA editing. Pol β functions in processes related to DNA repair (Beard and Wilson, 2006). The original description of the structure of Pol β (Pelletier et al., 1994) introduced a domain notation in which the Fingers and Thumb designations are flipped with respect to the notation used in this paper. Our designation of the Fingers and Thumb domains of Pol β corresponds with the domain notation used for canonical DNA polymerases after superposition of the DNA bound at the active site.

Pol III and Pol C constitute the C family of polymerases that are unique in terms of sequence. In order to help resolve the uncertainty concerning the evolutionary origins of the bacterial replicative DNA polymerases and to define the structural features that facilitate very high speed DNA synthesis, we have determined the structure of the catalytic α subunit of *E. coli* DNA Polymerase III. Although much of the chain fold is unrelated to that of other polymerases, the structure contains clearly recognizable Fingers, Thumb, and Palm domains. The Palm domain of Pol III is similar to that of X family polymerases, and it is likely that Pol III and Pol β are related evolutionary. Intriguingly, additional structural elements in the Palm domain of Pol III but not Pol β point to a much more distant relationship between Pol III and the A family DNA polymerases, such as Pol I. The Pol III structure allows us to model how the catalytic subunit interacts with DNA, the sliding clamp, and the 3′-5′ editing exonuclease.

RESULTS AND DISCUSSION

Overall Structure of Pol III

The crystal structure of a large fragment of Pol III (residues 1–917) was determined at 2.3 Å (Experimental Procedures). Based on analogy to a cupped right hand, the structure of Pol III consists of Fingers, Palm, and Thumb domains that together constitute the catalytic core of the enzyme (Figure 1). The detailed structural topology of Pol III is quite different from that of any known polymerase, except for specific localized features within the Palm domain. Pol III has a much larger Fingers domain than is typically seen, as well as a PHP (Polymerases and Histidinol Phosphatase) domain.

The heart of the protein is formed by the Palm domain (residues 271–432 and 511–560). The Fingers domain (residues 561–911) is located on the left side of the Palm domain in the reference view shown in Figures 1A and 1B. Four subdomains can be assigned within the extended Fingers domain of Pol III, and these are named the index (residues 641–756), middle (561–640 and 757–778), ring (779–838), and little Finger (839–911) subdomains.

The Thumb domain (residues 433–510) is located at the right side of the Palm domain and arches above it. Together, the Palm, Thumb, and Fingers domains form a deep cleft whose dimensions can readily accommodate duplex DNA such that it interacts with the active site located at the bottom of the cleft. The barrel-shaped PHP domain (residues 2–270) is located in the arch of the wrist, adjacent to the Thumb domain. The C-terminal segment of full-length Pol III, including the oligonucleotide binding (OB) fold and the two contact sites to the sliding clamp (Dohrmann and McHenry, 2005; Lopez de Saro et al., 2003), is not present in the structure but would connect to the extreme end of the little finger subdomain.

Similarity between the Active Sites of Pol III and DNA Polymerase β

The Palm domain is the most extensive contiguous region of high-sequence conservation on the surface of Pol III (Figure 5C and Figure S3). Located within a 5-stranded β sheet of the Palm domain are three strictly conserved

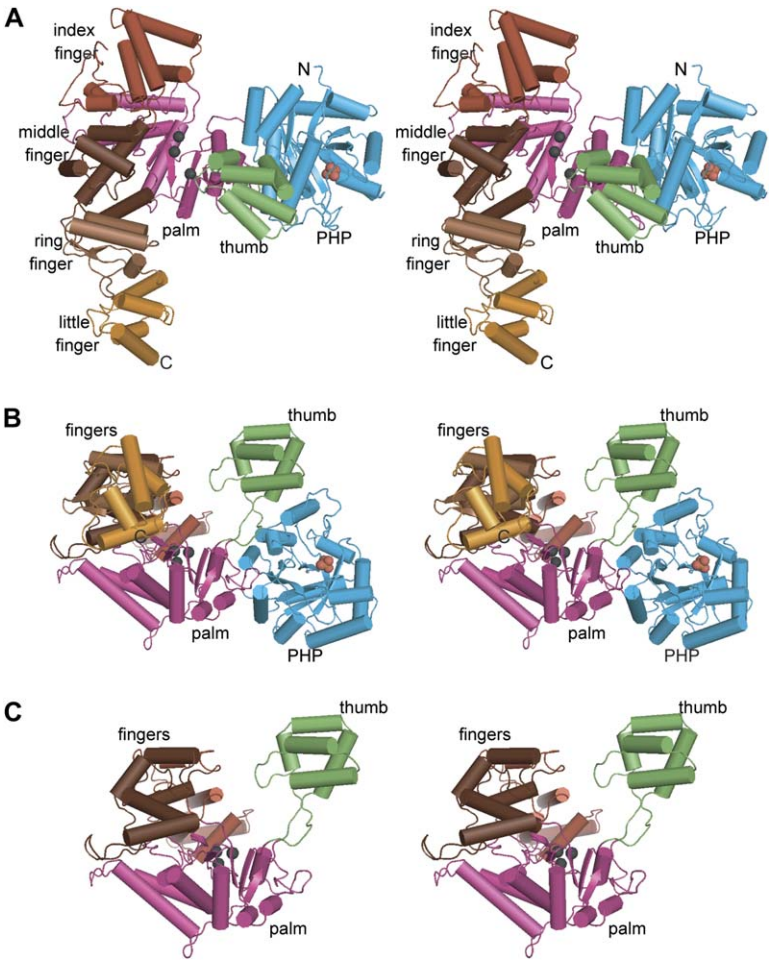

Figure 1. Overview of DNA Pol III Structure

(A) Top view in stereo and (B) side view in stereo. The location of the active site residues in the Palm domain are indicated by black spheres and the location of the phosphate ion in the PHP domain by red spheres. (C) The core region of Pol III alone resembles a cupped righthand shape. (PHP domain and ring and little Finger subdomains removed.)

aspartate residues (Asp401, Asp403, and Asp555) that are essential for catalysis (Pritchard and McHenry, 1999) (Figure 2B).

The Palm domains in A/B/Y family DNA polymerases each contain an antiparallel β sheet that presents three residues, typically aspartates, that form a catalytic triad

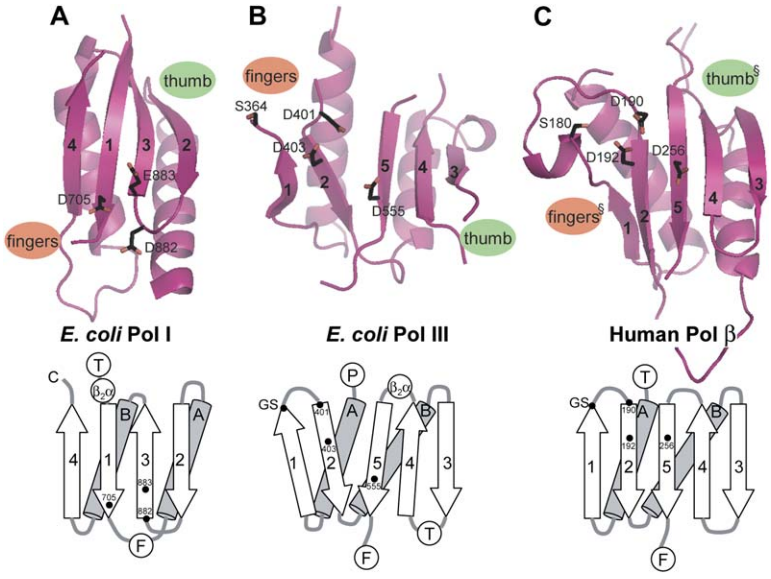

Figure 2. The Pol III Active Site Is Similar to that of Pol β

Close up of the active sites of (A) *E. coli* Pol I (Beese et al., 1993); PDB code 1KLN, (B) *E. coli* Pol III, (C) human Pol β (Sawaya et al., 1997); PDB code 1BPY. The view is similar to that of Figure 1A. The catalytic aspartates are indicated as black sticks. A topology diagram for each Palm domain is given below. The other domains are indicated as F (Fingers), T (Thumb), P (PHP), and $\beta_2\alpha$ motif. §Domain annotation for Pol β has been flipped to be consistent with that of canonical DNA polymerases.

(see Figure 2A). Two of the aspartates are involved in the coordinating of the two Mg^{2+} ions that are critical to the phosphotransferase mechanism, while the third aspartate (sometimes replaced by a glutamate, serine, or tyrosine) acts as a general base to activate the 3′ OH of the primer strand for nucleophilic attack on the α phosphate group of the incoming nucleotide (Brautigam and Steitz, 1998).

The Palm domain of the X family polymerases also contains a β sheet, but the antiparallel nature of the sheet is disrupted by an extra β strand that is inserted in the middle of the sheet (Figure 2C) (Davies et al., 1994; Pelletier et al., 1994). Although the X family polymerases also contain a triad of aspartate residues, the location of the catalytic triad is shifted from the "front" edge of the β sheet to the "back" edge of the β sheet (Figure 2). The order of the aspartates is also inverted, with the two nearby aspartates being separated by a single residue (DxD, rather than DD), and located 50–90 residues upstream rather than downstream from the third aspartate.

The structure of the Pol III active site is quite different from that of the A/B/Y polymerases and is similar to that of Pol β. In the A family polymerases, the strand order in the β sheet of the Palm domain is 4-1-3-2 (Figure 2A). In Pol III and Pol β, the strand order is different (1-2-5-4-3) (Figures 2B and 2C). The pattern of aspartates in Pol III (two on the second strand and one on the fifth) as well as their location near the back of the sheet rather than the front edge make the order of the catalytic aspartates in Pol III similar to that of Pol β. The similarity in the spacing of the aspartate residues in Pol III and Pol β has been noted earlier (Pritchard and McHenry, 1999).

The relationship between Pol III and Pol β is validated by the results of a structural similarity search using the DALI database (Holm and Sander, 1993). The top five matches to the Palm domain of Pol III are all nucleotidyltransferases, with human Pol β as the closest structural match. The rmsd between the Palm domains of Pol β and Pol III is 3.1 Å over 74 aligned Cα atoms.

In X family polymerases a conserved GS motif (Gly179 and Ser180 in human Pol β; Ser180 forms a hydrogen bond with the phosphate tail of the incoming nucleotide) is separated by 7–11 residues from the first two of the three catalytic aspartates (Asp190 and Asp192; the DxD motif) which are followed by the single aspartate (residue 256), 50–90 residues downstream (Figure 2C). Pol III does indeed have a conserved GS motif (residues 363–364) (Figure 2B), but it is separated from the DxD motif by 37 residues rather than 7–11. The DxD motif in Pol III (residues 401–403) is separated from the third aspartate (Asp555) by ~150 residues rather than 50–60, because the Thumb domain in Pol III is inserted between β strands 3 and 4 of the Palm domain. These strands are simply connected by a loop in Pol β. These differences in spacing between the conserved motifs explain why Pol III was not identified in a search for Pol β-related sequences (Aravind and Koonin, 1999).

The configuration of the three catalytically important aspartate residues in Pol III is different from that seen for the catalytic triad in Pol β and other nucleotidyltransferases. This difference is a consequence of the two β strands (2 and 5) that present the catalytic residues in Pol III being twisted apart by ~20°, with an accompanying buckling of the β sheet. Tyrosine 276 is wedged in between the two strands, while several bulky hydrophobic residues (i.e., Phe402 and Phe554) on the interior surface of the β sheet in Pol III make contact with residues in helices A and B that are located below and contribute to the buckling of the β sheet.

Pol III Cannot Bind DNA in a Pol β-like Manner

The binding mode of duplex DNA to X family polymerases is highly conserved, with the base pairs aligned parallel to the direction of the β strands of the Palm domain (Garcia-Diaz et al., 2004; Pelletier et al., 1994). We superimposed the structure of DNA bound human Pol β (Sawaya et al., 1997) onto the structure of Pol III (Figures 3A and 3B), using the catalytic triads and the β strands of the Palm domain as references. When this is done, the DNA of Pol β runs directly into a short α helix in Pol III (residues 543–549) that is located on top of the Palm domain (Figures 3B and 3D). The DNA is also blocked by the Thumb domain, which in Pol III has moved to the front side of the Palm domain in the view shown in Figure 2. The short α helix interacts tightly with the β sheet of the Palm domain in Pol III through several hydrophobic residues, while the location of the Thumb domain is stabilized by the PHP domain. These intimate contacts make it unlikely that these domains could move sufficiently upon DNA binding so as to accommodate a Pol β-like engagement of the DNA.

The $\beta_2\alpha$ Motif that Blocks Pol β-like DNA Binding Connects Pol III to A Family Polymerases

The helix that blocks the path of the DNA in Pol III is part of a $\beta_2\alpha$ structural motif, consisting of a β hairpin and the short α helix, which is inserted between strands 4 and 5 of the Palm domain (Figure 3D). The sequence of this structural element is conserved in the C family polymerases (Figure S2) but is not present in any member of the X family.

The $\beta_2\alpha$ motif in Pol III suggests an intriguing connection between Pol III and the A family polymerases such as Pol I, which have a similar motif in the Palm domain (B family polymerases, however, do not). In both Pol I and Pol III the Palm consists of two segments separated by the insertion of the Fingers (in Pol I) or the Thumb (in Pol III) (Figures 3C, 3D, and 3E). This is in contrast to Pol β, in which the Palm is one contiguous domain (Figures 2C and 3E). The smaller segment of the Palm domain ($Palm^S$) in both Pol I and Pol III contains the β strand that presents the third catalytic residue (Asp705 in strand 1 of *E. coli* Pol I and Asp555 in strand 5 of Pol III) and is flanked by the $\beta_2\alpha$ motif and the Fingers domain (Figure 3E). In Pol I and Pol III, the α helix of the $\beta_2\alpha$ motif is placed on top of the β sheet of the Palm domain, while the β hairpin is located adjacent to the sheet of the Palm domain and almost perpendicular to it (Figures 3C and 3D).

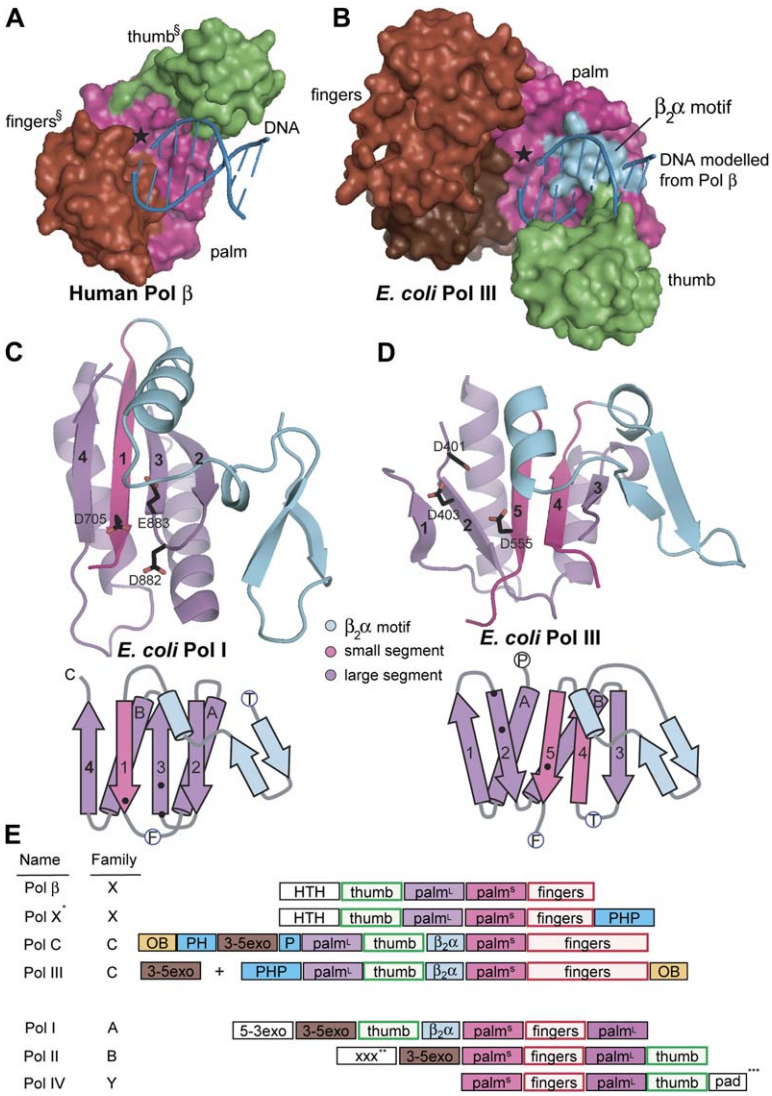

Figure 3. Pol III Palm Domain Cannot Bind DNA as Does Pol β and May Be Distantly Related to that of Pol I

(A) Top view of human Pol β bound to DNA (Sawaya et al., 1997); PDB code 1BPY. (B) Shown is the same view of Pol III with the DNA of Pol β placed into the structure. The modeled DNA runs into the helix of the $\beta_2\alpha$ motif on top of the Palm domain (blue) and the stem of the Thumb domain (green). For clarity the PHP domain and ring and little Fingers subdomains have been removed. The star indicates the position of the active site in Pol β and Pol III. (C) Ribbon diagram of the Palm domain of Pol I (Beese et al., 1993), PDB code 1KLN, and (D) Pol III with the $\beta_2\alpha$ motif is indicated in blue. A topology diagram of each is shown, with the two segments of the Palm domain colored differently. (E) The domain organizations of different DNA polymerases are shown. Domains with similar structures between polymerases families are colored in full colors. Domains with similar functions but different structures have the outline colored (i.e., Thumb and Fingers domain). Domains that are not related by function are colored in black and white. §Domain annotation for Pol β has been flipped to be consistent with the domain annotation of Pol I and Pol III. * indicates Bacterial Pol X. **Pol II has an N-terminal domain of unclear function. *** indicates "Polymerase Associated Domain," also called "Wrist" or "little Finger domain."

The secondary structural topology of the larger segment of the Palm domain ($Palm^L$) in both Pol I and Pol III is $\alpha\beta\beta^{**}\alpha\beta$, where α stands for α helix, β stands for β strand, and β^{**} indicates the strand that contains the two catalytic residues of the active site (Asp882 and Asp883 in strand 3 of *E. coli* Pol I and Asp401 and Asp403 in strand 2 of Pol III). The two segments of the Palm domain of Pol I and Pol III are, however, swapped in terms of their location in the sequence. The larger segment is N-terminal to the smaller segment in Pol I, whereas it is C-terminal to the smaller segment in Pol III (Figure 3E).

Figure 3E emphasizes the mosaic nature of the DNA polymerases and shows how Pol III and Pol C clearly group with the X family polymerases because of the similarities in the Palm domains. Note, however, that the presence of the $\beta_2\alpha$ motif immediately upstream of the smaller Palm segment ($Palm^S$) connects Pol III to Pol I (the A family). If Pol III is related, albeit very distantly, to Pol, I then Figures 3C and 3D indicate that their $Palm^L$ and $Palm^S$ segments would have had to have swapped places in the sequences, and, in terms of the three-dimensional structure, this swap would have been accompanied by a 180° rotation of one of the segments with respect to the other. Such a rearrangement is perhaps not extraordinary, given the extensive domain shuffling seen in the comparison of polymerases.

The PHP Active Site Shows Similarity to RecJ Exonuclease and Type II Phosphatase

As predicted (Aravind and Koonin, 1998b), the PHP domain has a TIM barrel-like fold with a seven-stranded β barrel surrounded by seven helices. A long loop on top of the domain (residues 203–240) extends out from it and makes extensive contacts with the Thumb domain (Figure 4A). This loop also forms a lid over a shallow cavity to which a phosphate ion is bound in the crystal structure.

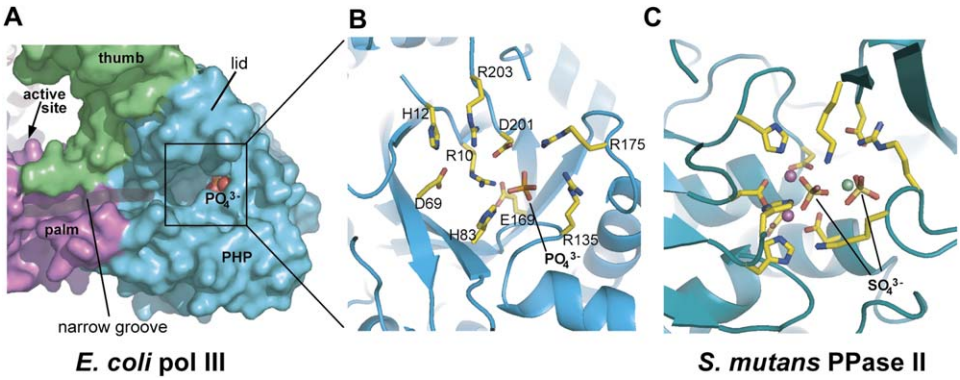

Figure 4. Pol III PHP Active Site Is Similar to that of DHH Phosphoesterases

(A) Surface representation showing PHP, Thumb, and Palm domains (similar view as in Figure 1B). A narrow groove runs from the Palm domain into a shallow cavity in the PHP domain that has phosphate bound. (B) Detailed view of shallow cavity in PHP domain is shown. (C) Active site of *Streptococcus mutans* PPase II (Merckel et al., 2001) is shown. Green sphere indicates a Mg^{2+} ion and purple spheres Mn^{2+} ions. The overall structure of this protein is unrelated to that of the PHP domain of Pol III.

A narrow but prominent groove formed by the lid and a second loop (residues 107–116) runs from the Palm domain into the shallow cavity, indicating a possible pathway for DNA to shuttle into the PHP active site (Figure 4A).

The shallow cavity corresponds to the active site in the crystal structures of two other PHP proteins, YcdX (Teplyakov et al., 2003) and Rnase P p30 subunit (Takagi et al., 2004), but the specific residues that make up the active site are very different in all three PHP domains. Unexpectedly, the configuration of active site residues in the Pol III PHP domain is similar to that seen in two members of the otherwise structurally unrelated DHH (Asp, His, His) superfamily (Aravind and Koonin, 1998a; Murzin et al., 1995), pyrophosphatase II (Merckel et al., 2001), and the 5′-3′ single-stranded exonuclease RecJ (Yamagata et al., 2002). These all have carboxylic acids located at the bottom of the cavity (Asp69, Glu169, and Asp201 in Pol III), two or three histidines needed for metal binding on one end (His12 and His83 in Pol III), and several positively charged residues on the opposite end of the active site (e.g., Arg135 and Arg175 in Pol III) (Figures 4B and 4C).

The PHP domain of Pol III has been proposed to act as a pyrophosphatase that hydrolyzes the pyrophosphate byproduct of DNA synthesis (Aravind and Koonin, 1998b). We have not, however, been able to detect any pyrophosphatase activity in Pol III (R.E.G., M.O.; data not shown). It has been shown recently that the PHP domain of *Thermus thermophilus* has 3′-5′ exonuclease activity and may function as an additional proofreading exonuclease (Stano et al., 2006).

A Model for DNA Binding to Pol III

Since Pol III cannot accommodate DNA in the manner observed in Pol β, we have been unable to use known crystal structures of polymerase-DNA complexes to model the binding of DNA to Pol III. Instead, we have placed a segment of standard B-form DNA into the Pol III active site and rotated the DNA into an orientation such that it does not overlap significantly with the protein (Figure 5A). Although speculative, the resulting model for DNA binding has several compelling features. The DNA is held between the Thumb and Fingers domains in a manner that resembles the interaction of other DNA polymerases with DNA. The DNA passes under the Thumb domain, which contacts the DNA backbone at the minor groove with several conserved and positively charged residues (Figure 5B). In addition, an arch of conserved positive residues runs from the Thumb domain into the Palm domain, following the backbone of the template strand (Figure S3).

The regions on the surface of Pol III that are predicted to interact with the DNA are highly conserved (Figure 5C and Figure S3). The pattern of sequence conservation at the surface also predicts a possible interaction site for the incoming nucleotide (Figure 5D). The 3′-terminal nucleotide and its template base come close to a loop connecting the index and middle Finger subdomains that is absolutely conserved in Pol III and Pol C. This loop (residues 753–758 in Pol III) is in a similar location as the template binding helix in other polymerases (termed the O helix in Pol I). The loop also contains two aromatic residues (Tyr754 and Phe756) that could potentially interact with the nascent base pair (Figure 5D). In addition, a patch of positive residues (e.g., Arg390, Arg396 in the Palm domain, and Arg709 and Arg710 in the index Finger subdomain) is located adjacent to the catalytic triad and appears to be well suited to interact with the negatively charged triphosphate tail of the incoming nucleotide (Figure 5D).

The C-Terminal Segment of Pol III Makes Extensive Interactions with the Sliding Clamp

All interactions between Pol III and the β-sliding clamp map to the C-terminal 243 residues of Pol III, which are not present in our crystal structure (Figure 6A). A β-clamp

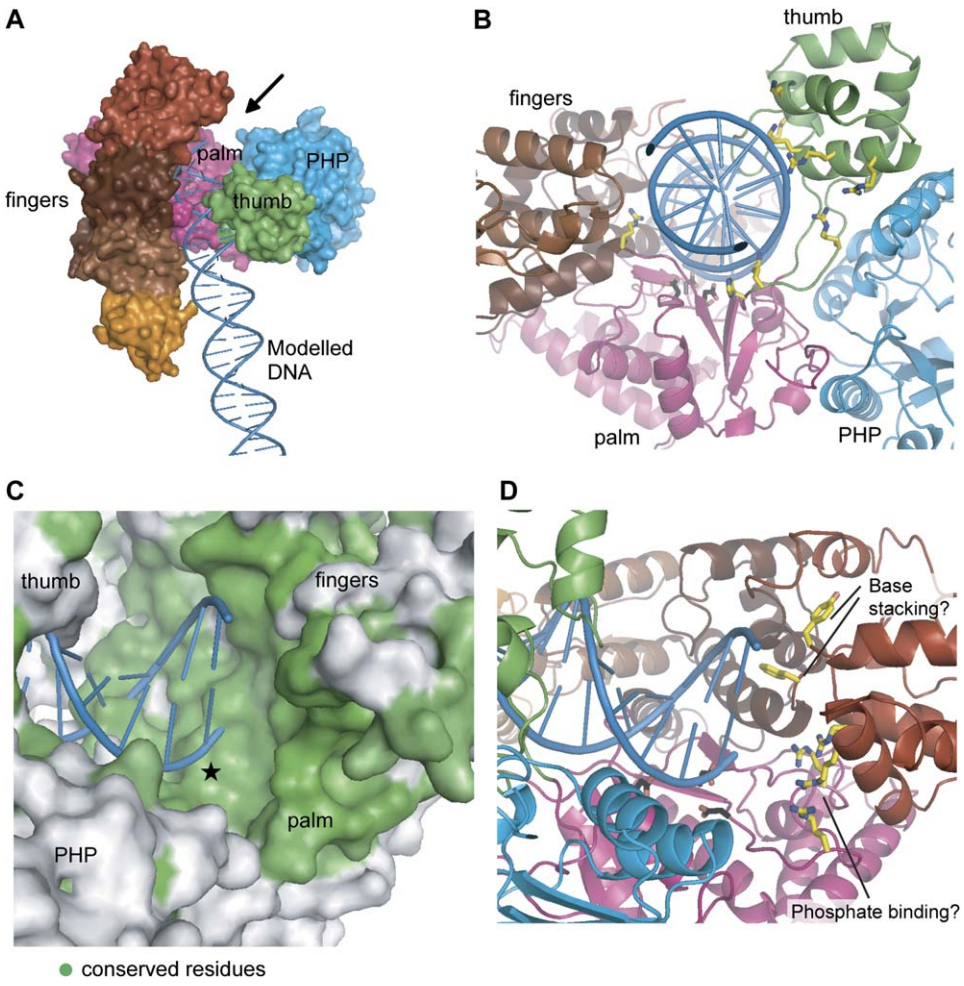

Figure 5. Model for DNA Binding in Pol III

(A) Surface representation of Pol III, with DNA indicated, is shown. The view is similar to that in Figure 1A. (B) Close up of the DNA-exit path, looking down the DNA axis, is shown. Several positively charged residues (colored in yellow) form an arch that contacts the backbone of the DNA. Active site residues are colored in black. (C) Close up view of a surface representation of the active site with conserved residues are represented in green. The viewpoint is along the arrow in panel (A). (D) Same view of the active site is shown with the catalytic triad in black sticks and residues that may be involved in nucleotide binding in yellow.

interaction motif is located at each end of this C-terminal segment. The first motif (residues 920–924) (Dohrmann and McHenry, 2005) is located just nine residues after the end of the crystal structure, while the second is located near the very C terminus of the full-length protein (residues 1154–1159) (Lopez de Saro et al., 2003). In addition, an OB domain (residues 994–1073) is located in the middle of the C-terminal segment, with strongest sequence similarity to the OB domain of the tRNA synthetase anticodon binding domain according to the PFAM database (Bateman et al., 2004). OB domains in other proteins are involved in protein-nucleic acid and protein-protein interaction (Theobald et al., 2003).

To further investigate the roles of the two β-clamp binding motifs and the OB domain we have generated a series of C-terminal deletion constructs of Pol III that were tested in a replication assay (Figure 6A). In this assay, singly primed M13 ssDNA coated with single-stranded DNA binding protein (SSB) is used to monitor DNA synthesis by the core subcomplex of the Pol III holoenzyme containing Pol III (the α subunit of the Pol III holoenzyme), the 3′-5′ exonuclease ε, and the θ subunit (a small domain of uncertain function). In the absence of the β clamp and clamp loader, Pol III core shows distributive rather than processive synthesis and is incapable of replicating the M13 DNA (Figure 6B and Figure S4). In the presence of the clamp and clamp loader, Pol III core shows highly processive DNA synthesis, replicating the 7.2 kb M13 DNA rapidly. When the extreme C-terminal β clamp binding motif is deleted (Pol III^{1121}, truncated at residue 1121), processive synthesis is still observed, albeit with less efficiency than for the wild-type Pol III core. When the OB domain

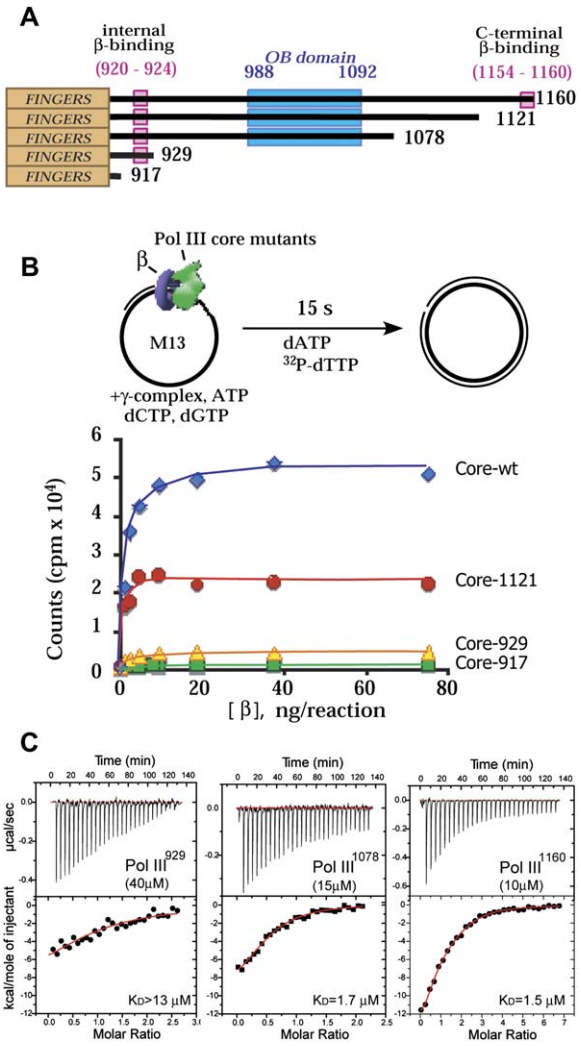

Figure 6. The C-terminal Region of Pol III, including the OB Domain, Is Required for β Stimulation

(A) Schematic diagram of the location of the β motifs in Pol III and the location of the deletions are shown. (B) Production of full-length M13 dsDNA after 20 s by core (Pol III, β clamp, ε exonuclease) complexes with different Pol III deletion constructs. (C) Isothermal titration calorimetry binding profile of clamp binding to full-length Pol III and deletion constructs. Time course radiograms are shown in Figure S4.

is also removed (Pol III^{929}), DNA replication becomes even less processive, showing no full-length 7.2 kb products even after 20 min (Figure S4). Finally, removal of the entire C-terminal segment (Pol III^{917}, the construct used for the crystal structure analysis) completely abolishes stimulation of replication by the β clamp. Overall, these experiments indicate that the OB domain cooperates with the clamp-recognition motifs for processive replication.

We have measured the strength of the interaction between the β clamp and various constructs of Pol III using isothermal titration calorimetry (ITC). The β clamp was titrated into a solution containing full-length or C-terminal deletion constructs of Pol III (Figure 6C). Full-length Pol III binds tightly to the β clamp (K_D=1.5 μM). When the C-terminal binding motif is removed, the affinity is essentially unchanged (K_D = 1.7 μM), but a marked decrease in affinity is observed when the OB domain is also deleted (K_D > 13 μM). Finally, when the internal β-clamp binding motif is also deleted, no binding to the clamp is detected (data not shown). Since these measurements are made in the absence of DNA, they indicate that the OB domain either interacts directly with the β clamp or helps present the internal β-clamp binding motif appropriately. These results suggest that the OB domain is located in the vicinity of the sliding clamp when the holoenzyme is assembled.

Building toward a Holoenzyme Structure

During replication, Pol III binds directly to the β clamp, the exonuclease ε, and the clamp loader subunit τ. Our model for Pol III core (Figure 7A) positions the β clamp close to the end of the Fingers domain, which fits well with the fact that the internal β-clamp binding site of Pol III begins nine residues after the end of our crystal structure. In this model, Pol III and β clamp span ~25 bp of DNA from the active site in Pol III to the exit of the clamp, consistent with the requirement of 22 or more bp for replication initiation by Pol III (Yao et al., 2000). In Pol C, the OB domain is located at the N terminus of the protein, preceding the PHP domain, rather than at the C-terminal end. Our model positions the β clamp between the end of the Fingers domain and the PHP domain, which allows for connection to the OB domain from either end.

In Pol C, the exonuclease domain is inserted into a loop (corresponding to residues 72–82 in Pol III) that connects the N- and C-terminal halves of the PHP domain (Figure 7B). The ε subunit of Pol III interacts with a region in Pol III that spans both the PHP and Palm domains (residues 255–320 [Wieczorek and McHenry, 2006]), running along the bottom of the polymerase structure (Figure 7B). This suggests that the exonuclease may bind in front of the Palm and PHP domains, under the exit path of the DNA and consistent with the observation that ε stimulates the interaction of Pol III with the β clamp (Studwell and O'Donnell, 1990).

This model suggests that the newly generated duplex DNA segment runs along the edge of the extended Fingers domain before it enters the central pore of the β clamp. Analysis of sequence conservation and electrostatic potential suggests that several residues in the ring and little Finger subdomains (e.g., residues Lys839, Arg876, and Arg877) are well positioned to make contact with the DNA prior to its engagement by the clamp (Figure S3). It is also possible that the OB domain makes contact with the DNA at the mouth of the clamp. Basic residues that are in the vicinity of RNA in structures of OB:RNA complexes are conserved in Pol III (e.g., Arg1004, Lys1009, and Arg1010).

These features suggest that Pol III and the sliding clamp together generate a channel that can hold the DNA in a loose but multifaceted embrace. The most intimate

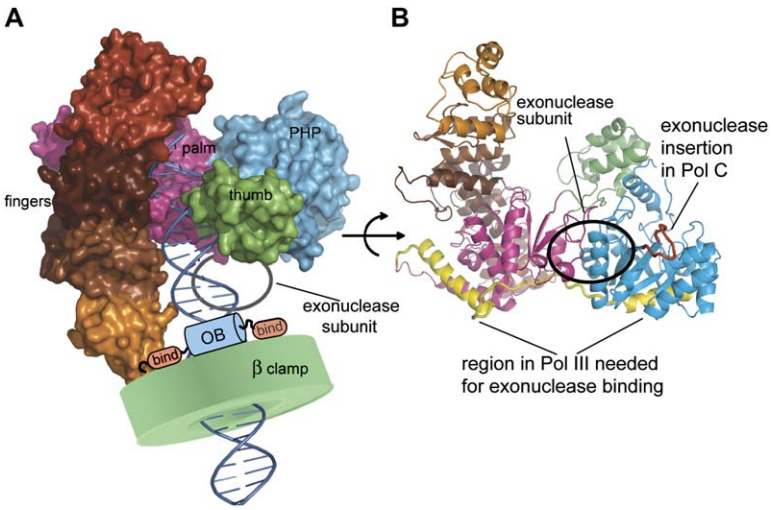

Figure 7. Model of Pol III Binding to DNA, Sliding Clamp β, and Exonuclease ε

(A) Surface representation of polymerase and DNA, with C-terminal region of Pol III and sliding clamp β indicated schematically, is shown. (B) Interaction sites of exonuclease ε binding to Pol III, with ε binding region in Pol III (Wieczorek and McHenry, 2006) colored in yellow and position of exonuclease insertion in Pol C in red.

contact with DNA is likely to occur at the site of nucleotide addition, but Pol III is expected to cycle through conformational changes that open and close the region around the active site. The structural features that are unique to Pol III thus appear to provide a means of minimizing complete disengagement from the DNA as the polymerase goes through thousands of processive cycles of nucleotide addition.

CONCLUSION

In this paper we show that the active sites of the bacterial replicative polymerases are closely related to those of Pol β and other members of the X family of DNA polymerases rather than to eukaryotic and archaeal replicative DNA polymerases. DNA Pol β is specialized for the incorporation of only a few nucleotides at a time and has limited fidelity when compared to the A and B family polymerases (Beard and Wilson, 2006). These functional attributes contrast sharply with the high fidelity and processivity that are the hallmark of Pol III function. The close similarity between the catalytic centers of Pol III and Pol β is therefore unexpected.

The marked dissimilarity in structure between the bacterial replicative DNA polymerases and the archaeal and eukaryotic replicative DNA polymerases lends additional support for the concept that the bacterial replicative DNA polymerases were selected independently, subsequent to the divergence of the bacteria from archaeal and eukaryotic lineages (Forterre, 2006; Leipe et al., 1999). One plausible route for the independent evolution of DNA replication systems is that the DNA polymerases first evolved in viruses, which then, in separate events, invaded the different branches of life after the split from a common ancestor with an RNA genome (Forterre, 2006).

The structure of Pol III also suggests a possible, although much more distant, evolutionary connection between the X family polymerases and the canonical DNA polymerases. This link is provided by the $\beta_2\alpha$ motif seen in the Palm domain of Pol III and in the A family polymerases (but not in X or B family members). Many nucleotidyltransferases operate on RNA, and reverse transcriptases are related to A family DNA polymerases. A common ancestor for all DNA polymerases may therefore have originated in the RNA world.

Perhaps the most remarkable distinguishing feature of bacterial DNA replication is its speed. Our structure of Pol III provides the first glimpse of how the catalytic subunit might be integrated with the sliding clamp to act processively on DNA. The next stage in our understanding of high-speed DNA replication awaits the determination of the structure of Pol III in complex with DNA and the sliding clamp.

EXPERIMENTAL PROCEDURES

Crystallization and Structure Determination of Pol III^{917}

Small angle X-ray scattering (SAXS) data for full-length *E. coli* Pol III were collected on the SIBYLS beamline 12.3.1 at the Advanced Light Source, Berkeley, CA (Figure S1), and three-dimensional shape reconstructions were obtained using Gasbor (Svergun et al., 2001). The low-resolution shape reconstructions showed a main body with a long and apparently flexible region protruding from it (Figure S1). A C-terminal deletion construct truncated after residue 917 (Pol III^{917}), which was based on a sequence alignment of 40 Pol III sequences, no longer showed evidence for the protruding region in the SAXS reconstructions (Figure S1), and this construct was crystallized under several conditions.

E. coli Pol III^{917} was expressed in BL21 (DE3) pLysS at 30°C for 1–2 hr at a starting OD600 of ~1 and purified using a method adapted from a previously published procedure (Maki and Kornberg, 1985). Briefly, supernatants of cell lysates were purified using Fast Flow Q, Heparin, MonoQ, and S200 gelfiltration columns. Purified protein was concentrated to 15–20 mg/ml, flash frozen, and stored at −80°C. Selenium-derivatized protein was expressed as described (Studier, 2005). Crystals (space group $P2_12_12_1$, see Table S1) were grown from protein at 15 mg/ml mixed with 15%–20% PEG3350, 0.2–0.4 M NaH2PO4, 100 mM HEPES, pH 7.5. Crystals were frozen in mother liquor including 20% glycerol.

A 3 wavelength MAD (multiple-wavelength anomalous diffraction) data set to 3.1 Å was collected at beamline 8.2.1 at the Advanced Light Source, Berkeley, CA. All data were processed with HKL2000 (Otwinowski and Minor, 1997). The locations of selenium sites were found with SHELXD (Schneider and Sheldrick, 2002) using the peak wavelength data set only. The sites were refined in SHARP (Bricogne et al., 2003) using all three wavelengths of the MAD data set. A higher-resolution data set to 2.6 Å was collected at beamline 8.3.1 and phase extension to 2.6 Å was performed using RESOLVE (Terwilliger, 2000), producing a map in which the larger part of the molecule could be traced. A large flexible segment of the structure (residues ~600–917) could only be built using electron density maps produced with BUSTER-TNT (Blanc et al., 2004), with model improvement by simulated annealing using CNS (crystallography and NMR system) (Brunger et al., 1998). A third data set to 2.3 Å was collected after controlled dehydration using the Free Mounting System (Rigaku) at the SIBYLS beamline 12.3.1 at the Advanced Light Source. This data set showed significant shrinkage in unit cell dimensions (from a = 83.7 Å, b = 100.7 Å, c = 143.7 Å to a = 83.7 Å, b = 94.0 Å, c = 131.2 Å) and the resulting electron density map was much improved, particularly for the flexible segment. Except for a ~5° rotation of the flexible segment no significant structural changes were observed. The model was built using O (Jones et al., 1991) and Coot (Emsley and Cowtan, 2004) and refined using Refmac5 with the TLS option (Winn et al., 2001). The final model (R_{work} = 19.7%, R_{free} = 26.5%) spans residues 2–911. Complete statistics for the model are in Table S1. Figures were prepared using Pymol (www.pymol.org).

Primed M13mp18 ssDNA Extension Assays

Replication assays were performed in 25 μl reactions containing 30 fmol of M13mp18 ssDNA primed with a 30-mer ssDNA, 0.8 μg SSB, 0.5 mM ATP, 60 μM dCTP, 60 μM dGTP, 740 fmol of β clamp, 20 fmol of clamp loader, and 0.5 pmol Pol III or mutant Pol III cores. Pol III core was reconstituted by incubating 0.5 pmol (Pol III wild-type and its truncations at residues 917, 929, 1078, and 1121, to which ε and θ subunits were added in 1:1.5 ratio) and preincubated 5 min at 37°C. Replication reaction was started upon addition of dATP and [α-^{32}P] dTTP to final concentrations of 60 and 20 μM, respectively. For time course reactions (Figure S4) the replication times are indicated in the Figure S4, and reactions were quenched upon addition of an equal volume of 1% SDS/40 mM EDTA. Products were analyzed in a 0.8% agarose gel in 1 × TBE. For Pol III replication reactions, various amounts of β clamp were used (0–740 pmoles), and reactions were quenched after 15 s by spotting reactions on DEAE-cellulose circles (Whatman) followed by washing and counting in a liquid scintillation counter.

Isothermal Titration Calorimetry Experiments

Binding studies were performed by isothermal titration calorimetry (ITC) using a VP-ITC microcalorimeter (MicroCal, Northampton, MA). β clamp and Pol III (Pol III^{929}, Pol III^{1078}, Pol III^{1160}) were dialyzed extensively against 20 mM Hepes buffer pH 7.5, 0.5 mM EDTA, and 50 mM NaCl. The reaction cell (1.4 ml) was filled with degassed solutions and equilibrated at 25°C. Stirring speed was 400 rpm, the thermal power was recorded every second, and instrumental feedback (reference power) was 10%. In a typical experiment, β clamp (100–220 μM in the syringe) was titrated over 28 injections of 10 μl into the cell containing 10–40 μM solution of purified Pol III^{1160} or its truncations. An initial injection of 2 μl was made before each titration to ensure that the titrant (β clamp) concentration was at its loading value. The heats of dilution were obtained at 25°C from separate titration experiments of β clamp into buffer. The corrected quantity of heat released due to β clamp binding to Pol III and Pol III deletion constructs was measured by integrating the area of each titration peak. Calculation of binding enthalpy, entropy, and stoichiometry from protein titration data was accomplished using ORIGIN software (Microcal).

Supplemental Data

Supplemental Data include four figures and two tables and can be found with this article online at http://www.cell.com/cgi/content/full/126/5/881/DC1/.

ACKNOWLEDGMENTS

We thank the staff at beamlines 8.2.1, 8.2.2, 8.3.1, and 12.3.1 of the Advanced Light Source, Berkeley, CA, for their help and technical support. We are thankful to Clemens Vonrhein for help with BUSTER-TNT, Axel Brunger for help with CNS, and Anastassis Perrakis for helpful suggestions. We thank members of the Kuriyan laboratory, particularly Joel Guenther, Steven Kazmirsky, and Xuewu Zhang for help and advice. This work was supported in part by grants from the NIH to J.K. (GM45547) and M.O. (GM38839). M.H.L. was supported by a Jane Coffin Childs Memorial Fund Fellowship.

Received: May 16, 2006
Revised: June 29, 2006
Accepted: July 29, 2006
Published: September 7, 2006

REFERENCES

Aravind, L., and Koonin, E.V. (1998a). A novel family of predicted phosphoesterases includes Drosophila prune protein and bacterial RecJ exonuclease. Trends Biochem. Sci. *23*, 17–19.

Aravind, L., and Koonin, E.V. (1998b). Phosphoesterase domains associated with DNA polymerases of diverse origins. Nucleic Acids Res. *26*, 3746–3752.

Aravind, L., and Koonin, E.V. (1999). DNA polymerase beta-like nucleotidyltransferase superfamily: identification of three new families, classification and evolutionary history. Nucleic Acids Res. *27*, 1609–1618.

Bateman, A., Coin, L., Durbin, R., Finn, R.D., Hollich, V., Griffiths-Jones, S., Khanna, A., Marshall, M., Moxon, S., Sonnhammer, E.L., et al. (2004). The Pfam protein families database. Nucleic Acids Res. *32*, D138–D141.

Beard, W.A., and Wilson, S.H. (2006). Structure and mechanism of DNA polymerase Beta. Chem. Rev. *106*, 361–382.

Beese, L.S., Derbyshire, V., and Steitz, T.A. (1993). Structure of DNA polymerase I Klenow fragment bound to duplex DNA. Science *260*, 352–355.

Blanc, E., Roversi, P., Vonrhein, C., Flensburg, C., Lea, S.M., and Bricogne, G. (2004). Refinement of severely incomplete structures with maximum likelihood in BUSTER-TNT. Acta Crystallogr. D Biol. Crystallogr. *60*, 2210–2221.

Bloom, L.B., Chen, X., Fygenson, D.K., Turner, J., O'Donnell, M., and Goodman, M.F. (1997). Fidelity of Escherichia coli DNA polymerase III holoenzyme. The effects of beta, gamma complex processivity proteins and epsilon proofreading exonuclease on nucleotide misincorporation efficiencies. J. Biol. Chem. *272*, 27919–27930.

Bonner, C.A., Hays, S., McEntee, K., and Goodman, M.F. (1990). DNA polymerase II is encoded by the DNA damage-inducible dinA gene of Escherichia coli. Proc. Natl. Acad. Sci. USA *87*, 7663–7667.

Bowman, G.D., Goedken, E.R., Kazmirski, S.L., O'Donnell, M., and Kuriyan, J. (2005). DNA polymerase clamp loaders and DNA recognition. FEBS Lett. *579*, 863–867.

Braithwaite, D.K., and Ito, J. (1993). Compilation, alignment, and phylogenetic relationships of DNA polymerases. Nucleic Acids Res. *21*, 787–802.

Brautigam, C.A., and Steitz, T.A. (1998). Structural and functional insights provided by crystal structures of DNA polymerases and their substrate complexes. Curr. Opin. Struct. Biol. *8*, 54–63.

Bricogne, G., Vonrhein, C., Flensburg, C., Schiltz, M., and Paciorek, W. (2003). Generation, representation and flow of phase information in structure determination: recent developments in and around SHARP 2.0. Acta Crystallogr. D Biol. Crystallogr. *59*, 2023–2030.

Bruck, I., Goodman, M.F., and O'Donnell, M. (2003). The essential C family DnaE polymerase is error-prone and efficient at lesion bypass. J. Biol. Chem. *278*, 44361–44368.

Brunger, A.T., Adams, P.D., Clore, G.M., DeLano, W.L., Gros, P., Grosse-Kunstleve, R.W., Jiang, J.S., Kuszewski, J., Nilges, M., Pannu, N.S., et al. (1998). Crystallography & NMR system: A new software suite for macromolecular structure determination. Acta Crystallogr. D Biol. Crystallogr. *54*, 905–921.

Davies, J.F., II, Almassy, R.J., Hostomska, Z., Ferre, R.A., and Hostomsky, Z. (1994). 2.3 A crystal structure of the catalytic domain of DNA polymerase beta. Cell *76*, 1123–1133.

Dohrmann, P.R., and McHenry, C.S. (2005). A bipartite polymerase-processivity factor interaction: only the internal beta binding site of the alpha subunit is required for processive replication by the DNA polymerase III holoenzyme. J. Mol. Biol. *350*, 228–239.

Doublie, S., Tabor, S., Long, A.M., Richardson, C.C., and Ellenberger, T. (1998). Crystal structure of a bacteriophage T7 DNA replication complex at 2.2 A resolution. Nature *391*, 251–258.

Emsley, P., and Cowtan, K. (2004). Coot: model-building tools for molecular graphics. Acta Crystallogr. D Biol. Crystallogr. *60*, 2126–2132.

Eom, S.H., Wang, J., and Steitz, T.A. (1996). Structure of Taq polymerase with DNA at the polymerase active site. Nature *382*, 278–281.

Forterre, P. (2006). Three RNA cells for ribosomal lineages and three DNA viruses to replicate their genomes: a hypothesis for the origin of cellular domain. Proc. Natl. Acad. Sci. USA *103*, 3669–3674.

Franklin, M.C., Wang, J., and Steitz, T.A. (2001). Structure of the replicating complex of a pol alpha family DNA polymerase. Cell *105*, 657–667.

Garcia-Diaz, M., Bebenek, K., Krahn, J.M., Blanco, L., Kunkel, T.A., and Pedersen, L.C. (2004). A structural solution for the DNA polymerase lambda-dependent repair of DNA gaps with minimal homology. Mol. Cell *13*, 561–572.

Goodman, M.F. (2002). Error-prone repair DNA polymerases in prokaryotes and eukaryotes. Annu. Rev. Biochem. *71*, 17–50.

Holm, L., and Sander, C. (1993). Protein structure comparison by alignment of distance matrices. J. Mol. Biol. *233*, 123–138.

Holm, L., and Sander, C. (1995). DNA polymerase beta belongs to an ancient nucleotidyltransferase superfamily. Trends Biochem. Sci. *20*, 345–347.

Hopfner, K.P., Eichinger, A., Engh, R.A., Laue, F., Ankenbauer, W., Huber, R., and Angerer, B. (1999). Crystal structure of a thermostable type B DNA polymerase from Thermococcus gorgonarius. Proc. Natl. Acad. Sci. USA *96*, 3600–3605.

Huang, Y., Braithwaite, D.K., and Ito, J. (1997). Evolution of dnaQ, the gene encoding the editing 3′ to 5′ exonuclease subunit of DNA polymerase III holoenzyme in Gram-negative bacteria. FEBS Lett. *400*, 94–98.

Johnson, A., and O'Donnell, M. (2005). Cellular DNA replicases: components and dynamics at the replication fork. Annu. Rev. Biochem. *74*, 283–315.

Jones, T.A., Zou, J.-Y., Cowan, S.W., and Kjeldgaard, M. (1991). Improved methods for the building of protein models in electron density maps and the location of errors in these models. Acta Crystallogr. *A47*, 110–119.

Kiefer, J.R., Mao, C., Braman, J.C., and Beese, L.S. (1998). Visualizing DNA replication in a catalytically active Bacillus DNA polymerase crystal. Nature *391*, 304–307.

Kong, X.P., Onrust, R., O'Donnell, M., and Kuriyan, J. (1992). Three-dimensional structure of the beta subunit of E. coli DNA polymerase III holoenzyme: a sliding DNA clamp. Cell *69*, 425–437.

Krishna, T.S., Kong, X.P., Gary, S., Burgers, P.M., and Kuriyan, J. (1994). Crystal structure of the eukaryotic DNA polymerase processivity factor PCNA. Cell *79*, 1233–1243.

Leipe, D.D., Aravind, L., and Koonin, E.V. (1999). Did DNA replication evolve twice independently? Nucleic Acids Res. *27*, 3389–3401.

Li, Y., Korolev, S., and Waksman, G. (1998). Crystal structures of open and closed forms of binary and ternary complexes of the large fragment of Thermus aquaticus DNA polymerase I: structural basis for nucleotide incorporation. EMBO J. *17*, 7514–7525.

Lopez de Saro, F.J., Georgescu, R.E., and O'Donnell, M. (2003). A peptide switch regulates DNA polymerase processivity. Proc. Natl. Acad. Sci. USA *100*, 14689–14694.

Maki, H., and Kornberg, A. (1985). The polymerase subunit of DNA polymerase III of Escherichia coli. II. Purification of the alpha subunit, devoid of nuclease activities. J. Biol. Chem. *260*, 12987–12992.

Merckel, M.C., Fabrichniy, I.P., Salminen, A., Kalkkinen, N., Baykov, A.A., Lahti, R., and Goldman, A. (2001). Crystal structure of Streptococcus mutans pyrophosphatase: a new fold for an old mechanism. Structure *9*, 289–297.

Murzin, A.G., Brenner, S.E., Hubbard, T., and Chothia, C. (1995). SCOP: a structural classification of proteins database for the investigation of sequences and structures. J. Mol. Biol. *247*, 536–540.

Otwinowski, Z., and Minor, W. (1997). Processing of X-ray Diffraction Data Collected in Oscillation Mode. Methods Enzymol. *276*, 307–326.

Pelletier, H., Sawaya, M.R., Kumar, A., Wilson, S.H., and Kraut, J. (1994). Structures of ternary complexes of rat DNA polymerase beta, a DNA template-primer, and ddCTP. Science *264*, 1891–1903.

Pritchard, A.E., and McHenry, C.S. (1999). Identification of the acidic residues in the active site of DNA polymerase III. J. Mol. Biol. *285*, 1067–1080.

Raghuraman, M.K., Winzeler, E.A., Collingwood, D., Hunt, S., Wodicka, L., Conway, A., Lockhart, D.J., Davis, R.W., Brewer, B.J., and Fangman, W.L. (2001). Replication dynamics of the yeast genome. Science *294*, 115–121.

Rodriguez, A.C., Park, H.W., Mao, C., and Beese, L.S. (2000). Crystal structure of a pol alpha family DNA polymerase from the hyperthermophilic archaeon Thermococcus sp. 9 degrees N-7. J. Mol. Biol. *299*, 447–462.

Rothwell, P.J., and Waksman, G. (2005). Structure and mechanism of DNA polymerases. Adv. Protein Chem. *71*, 401–440.

Sawaya, M.R., Prasad, R., Wilson, S.H., Kraut, J., and Pelletier, H. (1997). Crystal structures of human DNA polymerase beta complexed with gapped and nicked DNA: evidence for an induced fit mechanism. Biochemistry *36*, 11205–11215.

Schneider, T.R., and Sheldrick, G.M. (2002). Substructure solution with SHELXD. Acta Crystallogr. D Biol. Crystallogr. *58*, 1772–1779.

Stano, N.M., Chen, J., and McHenry, C.S. (2006). A coproofreading Zn(2+)-dependent exonuclease within a bacterial replicase. Nat. Struct. Mol. Biol. *13*, 458–459.

Studier, F.W. (2005). Protein production by auto-induction in high density shaking cultures. Protein Expr. Purif. *41*, 207–234.

Studwell, P.S., and O'Donnell, M. (1990). Processive replication is contingent on the exonuclease subunit of DNA polymerase III holoenzyme. J. Biol. Chem. *265*, 1171–1178.

Svergun, D.I., Petoukhov, M.V., and Koch, M.H. (2001). Determination of domain structure of proteins from X-ray solution scattering. Biophys. J. *80*, 2946–2953.

Takagi, H., Watanabe, M., Kakuta, Y., Kamachi, R., Numata, T., Tanaka, I., and Kimura, M. (2004). Crystal structure of the ribonuclease

P protein Ph1877p from hyperthermophilic archaeon Pyrococcus horikoshii OT3. Biochem. Biophys. Res. Commun. *319*, 787–794.

Teplyakov, A., Obmolova, G., Khil, P.P., Howard, A.J., Camerini-Otero, R.D., and Gilliland, G.L. (2003). Crystal structure of the Escherichia coli YcdX protein reveals a trinuclear zinc active site. Proteins *51*, 315–318.

Terwilliger, T.C. (2000). Maximum-likelihood density modification. Acta Crystallogr. D Biol. Crystallogr. *56*, 965–972.

Theobald, D.L., Mitton-Fry, R.M., and Wuttke, D.S. (2003). Nucleic acid recognition by OB-fold proteins. Annu. Rev. Biophys. Biomol. Struct. *32*, 115–133.

Waga, S., and Stillman, B. (1998). The DNA replication fork in eukaryotic cells. Annu. Rev. Biochem. *67*, 721–751.

Wang, J., Sattar, A.K., Wang, C.C., Karam, J.D., Konigsberg, W.H., and Steitz, T.A. (1997). Crystal structure of a pol alpha family replication DNA polymerase from bacteriophage RB69. Cell *89*, 1087–1099.

Wieczorek, A., and McHenry, C.S. (2006). The NH2-terminal php domain of the alpha subunit of the Escherichia coli replicase binds the epsilon proofreading subunit. J. Biol. Chem. *281*, 12561–12567.

Winn, M.D., Isupov, M.N., and Murshudov, G.N. (2001). Use of TLS parameters to model anisotropic displacements in macromolecular refinement. Acta Crystallogr. D Biol. Crystallogr. *57*, 122–133.

Yamagata, A., Kakuta, Y., Masui, R., and Fukuyama, K. (2002). The crystal structure of exonuclease RecJ bound to Mn2+ ion suggests how its characteristic motifs are involved in exonuclease activity. Proc. Natl. Acad. Sci. USA *99*, 5908–5912.

Yao, N., Leu, F.P., Anjelkovic, J., Turner, J., and O'Donnell, M. (2000). DNA structure requirements for the Escherichia coli gamma complex clamp loader and DNA polymerase III holoenzyme. J. Biol. Chem. *275*, 11440–11450.

Zhao, Y., Jeruzalmi, D., Moarefi, I., Leighton, L., Lasken, R., and Kuriyan, J. (1999). Crystal structure of an archaebacterial DNA polymerase. Structure *7*, 1189–1199.

Accession Numbers

The structures described in our paper have been deposited in the Protein Data Bank under ID codes 2HQA and 2HNH.